ADVANCING EARTH AND SPACE SCIENCES

JGR Biogeosciences

RESEARCH ARTICLE

10.1029/2025JG009090

Key Points:

- Dissolved organic carbon (DOC) and alkalinity concentrations had contrasting seasonal and event-driven patterns in their relationships to streamflow
- DOC was delivered to streams mainly via shallow flowpaths during high flows, while alkalinity inputs were highest during low flows
- Changes in hydroclimate have the potential to impact dissolved carbon export through both seasonal shifts and patterns of storm events

Supporting Information:

Supporting Information may be found in the online version of this article.

Correspondence to:

C. Delbecq,
cedelbecq@alaska.edu

Citation:

Delbecq, C., Fellman, J. B., Bellmore, J. R., Whitney, E. J., Fitzgerald, K., & Falke, J. A. (2026). Season and antecedent conditions impact concentration-discharge relationships for dissolved organic carbon and alkalinity in a Southeast Alaskan watershed. *Journal of Geophysical Research: Biogeosciences*, *131*, e2025JG009090. https://doi.org/10.1029/2025JG009090

Received 26 JUN 2025
Accepted 11 DEC 2025

Author Contributions:

Conceptualization: Jason B. Fellman, J. Ryan Bellmore, Jeffrey A. Falke
Data curation: Claire Delbecq, Emily J. Whitney
Formal analysis: Claire Delbecq, Jason B. Fellman, Emily J. Whitney
Funding acquisition: Jason B. Fellman, J. Ryan Bellmore, Jeffrey A. Falke
Investigation: Claire Delbecq, Emily J. Whitney, Kevin Fitzgerald
Methodology: Jason B. Fellman, J. Ryan Bellmore, Jeffrey A. Falke
Resources: Jason B. Fellman, J. Ryan Bellmore, Jeffrey A. Falke
Supervision: Jason B. Fellman, J. Ryan Bellmore, Jeffrey A. Falke
Validation: Emily J. Whitney, Jeffrey A. Falke

Season and Antecedent Conditions Impact Concentration-Discharge Relationships for Dissolved Organic Carbon and Alkalinity in a Southeast Alaskan Watershed

Claire Delbecq[1], Jason B. Fellman[2,3], J. Ryan Bellmore[4], Emily J. Whitney[3], Kevin Fitzgerald[1], and Jeffrey A. Falke[5]

[1]College of Fisheries and Ocean Sciences, University of Alaska Fairbanks, Juneau, AK, USA, [2]Program on the Environment, University of Alaska Southeast, Juneau, AK, USA, [3]Alaska Coastal Rainforest Center, University of Alaska Southeast, Juneau, AK, USA, [4]U. S. Forest Service, Pacific Northwest Research Station, Juneau, AK, USA, [5]U. S. Geological Survey, Alaska Cooperative Fish and Wildlife Research Unit, Fairbanks, AK, USA

Abstract Fluvial export of dissolved carbon plays an important role in watershed-scale biogeochemistry. Predicted changes in climate are expected to impact watershed hydrologic regimes, and in turn, the sources and export of dissolved carbon from watersheds. Here, we utilize high resolution measurements of discharge and dissolved carbon concentration to examine how concentration-discharge (CQ) relationships vary seasonally and during high flow events over the main runoff season (May–October) in a temperate forested watershed in Southeast Alaska. Concentration-discharge relationships for dissolved organic carbon (DOC) and alkalinity demonstrated strong seasonal patterns, with more linear relationships in May and June versus other months. Changing power law model slopes (b values; the exponent in a power law regression between runoff and carbon yields) indicated potentially shifting watershed sources (biogenic vs. geologic) and contrasting dominant flowpaths (shallow vs. deeper groundwater) for DOC and alkalinity over the sampling period. During the largest storm event of the study, DOC and alkalinity b values shifted from an overall pattern of transport (mean $b = 1.58$ values >1.0 indicate transport limitation) and source limitation (mean $b = 0.48$, values <1.0 indicate source limitation) to chemostatic (DOC, $b = 0.99$; alkalinity, $b = 1.019$). In June through August, patterns in hysteresis index suggest that CQ relationships were altered when storms followed in close succession to each other. Together, these findings indicate that seasonal and antecedent flow conditions play a role in dissolved carbon export from forested watersheds. Understanding these dynamics, particularly during winter months, will become increasingly important as changes to hydroclimate impact riverine carbon export.

Plain Language Summary Rivers and streams transport dissolved carbon to the ocean, helping drive the global carbon cycle. Climate change is expected to alter rainfall, snowfall, and storm intensity, which may affect the amount and type of carbon exported from watersheds. To better predict these impacts, we need to understand how dissolved carbon concentrations change under different hydrologic conditions. In our study, we measured streamflow and dissolved organic carbon (DOC) and alkalinity (a proxy for inorganic carbon) concentrations from late April through October in a Southeast Alaska watershed. We found that the relationship between streamflow and carbon concentration varied by season. In spring, DOC and alkalinity levels increased steadily with streamflow, forming a strong linear relationship. In summer, the relationship was asymptotic, meaning carbon concentrations leveled off at high flows instead of continuing to rise. When analyzing individual storms, typically lasting about a day, we observed different patterns in how carbon concentrations changed as flow increased or decreased. Additionally, storms occurring within a few days of each other appeared to influence stream carbon levels in subsequent storms. Altogether, our findings indicate that seasonality and storm sequences play an important role in controlling dissolved carbon export from rivers and streams.

1. Introduction

Fluvial fluxes of different species of carbon play an important role in watershed carbon cycling (Aufdenkampe et al., 2011). In general, the dominant carbon species exported laterally from watersheds are dissolved organic (DOC) and inorganic carbon (DIC; Chaplot & Mutema, 2021), and strong evidence exists that watershed hydrology influences the relationship between discharge and DOC/DIC concentration and export (Ward et al., 2017). For example, high flow events can mobilize a large percentage of the total annual

Writing – original draft: Claire Delbecq
Writing – review & editing: Jason B. Fellman, J. Ryan Bellmore, Emily J. Whitney, Kevin Fitzgerald, Jeffrey A. Falke

watershed export of DOC (Raymond & Saiers, 2010; Wiegner et al., 2009), making storms important in the context of terrestrial carbon budgets and ecologically significant pulses of carbon to downstream ecosystems (Wilson et al., 2013). Shifting watershed hydrologic patterns, such as more frequent and intense storms and severe dry periods (e.g., Lader et al., 2020, 2022), have the potential to influence concentration-discharge (CQ) relationships and therefore watershed carbon budgets. Thus, future changes in hydroclimate underscore the importance of improving our understanding of the relationship between hydrologic patterns and fluvial carbon export (Tank et al., 2018).

Development of a mechanistic understanding of seasonal CQ relationships has been challenging because many estimates of streamwater dissolved carbon export have often relied on infrequent point measurements collected across years (e.g., Leach et al., 2016; Perdrial et al., 2014; Raymond & Saiers, 2010). Previous studies have typically been limited to a few storms (<10) over a short time frame (e.g., Hood et al., 2006; Jung et al., 2012; Su et al., 2023) making it difficult to understand how CQ relationships for individual storm events fit into broader seasonal trends. Additionally, little is known about how antecedent conditions (e.g., storms in close succession or periods of prolonged low flow) or highly seasonal flow regimes (e.g., spring snowmelt, summer low flow) impact the response of CQ relationships for any given storm (McMillan et al., 2018).

Over the past few decades, high quality optical sensors have been developed that can be deployed under variable weather and flow conditions making collection of high-resolution data over longer sampling periods more feasible (Downing et al., 2012; Saraceno et al., 2009; Vaughan et al., 2019). In situ sensors can be used to capture hourly measurements of fluorescent dissolved organic matter (FDOM, which can be related to DOC concentration), temperature, turbidity, conductivity, and other physicochemical properties. More recently, high-resolution specific conductivity measurements have been related to DIC concentrations (e.g., Koch et al., 2021) making it possible to address more nuanced questions around how storm sequencing and watershed antecedent conditions might impact multiple carbon species and the CQ response observed under different flow conditions (Koch et al., 2021; Wilson et al., 2013).

High-resolution carbon data and CQ indices can be combined to quantify changes in relationships between streamflow and carbon concentration and interaction among storm sequences. One basic CQ index is the power law relationship where the slope of the log(C) ~ log(Q) relationship or exponent in the power law regression (*b* value) indicates dissolved carbon is either source or transport limited within the watershed (Moatar et al., 2017; Zarnetske et al., 2018). Alternatively, metrics of hysteresis and loop direction (Speir et al., 2023; Williams, 1989) can provide insight into flowpaths and sources of dissolved carbon within the watershed, with clockwise (CW) hysteresis indicating the mobilization of proximate sources early in the storm and dilution later in the storm, and counterclockwise (CCW) hysteresis indicating mobilization of more distal sources later in the storm (Lloyd et al., 2016a). Although multi-year trends for single carbon species have been quantified (e.g., Zarnetske et al., 2018), high-resolution studies that assess CQ behavior of multiple species of carbon over a season and with many individual storm events are rare (except see Koch et al., 2021).

A combination of high rates of precipitation, variable flow conditions, and a carbon-rich landscape makes Southeast Alaska an ideal place to study the interactions between seasonal and storm event CQ relationships for different species of carbon (Bidlack et al., 2021). While few temperate regions experience the magnitude of precipitation common in Southeast Alaska, climate shifts are predicted to make storm series like those that occur in Southeast Alaska more common (Espinoza et al., 2018; Lader et al., 2020). Here, we use grab samples (at least weekly) of DOC and alkalinity concentrations and hourly measurements of florescent dissolved organic matter (FDOM) and specific conductivity to quantify hourly concentrations of DOC and alkalinity, respectively. Alkalinity is not a direct measurement of DIC; however, it is often assumed that the majority of alkalinity is DIC in forested watersheds (Cole et al., 2021). We used the hourly concentrations for DOC and alkalinity and simple metrics to describe concentration-discharge relationships to quantify seasonal and storm event trends in a forested watershed in Southeast Alaska over a 6-month study window. We pose two questions: (a) Is there an emergent relationship between concentrations of DOC and alkalinity and discharge for the entire sampling period? And if not, (b) how do these relationships between carbon species and discharge vary seasonally and during individual high flow events?

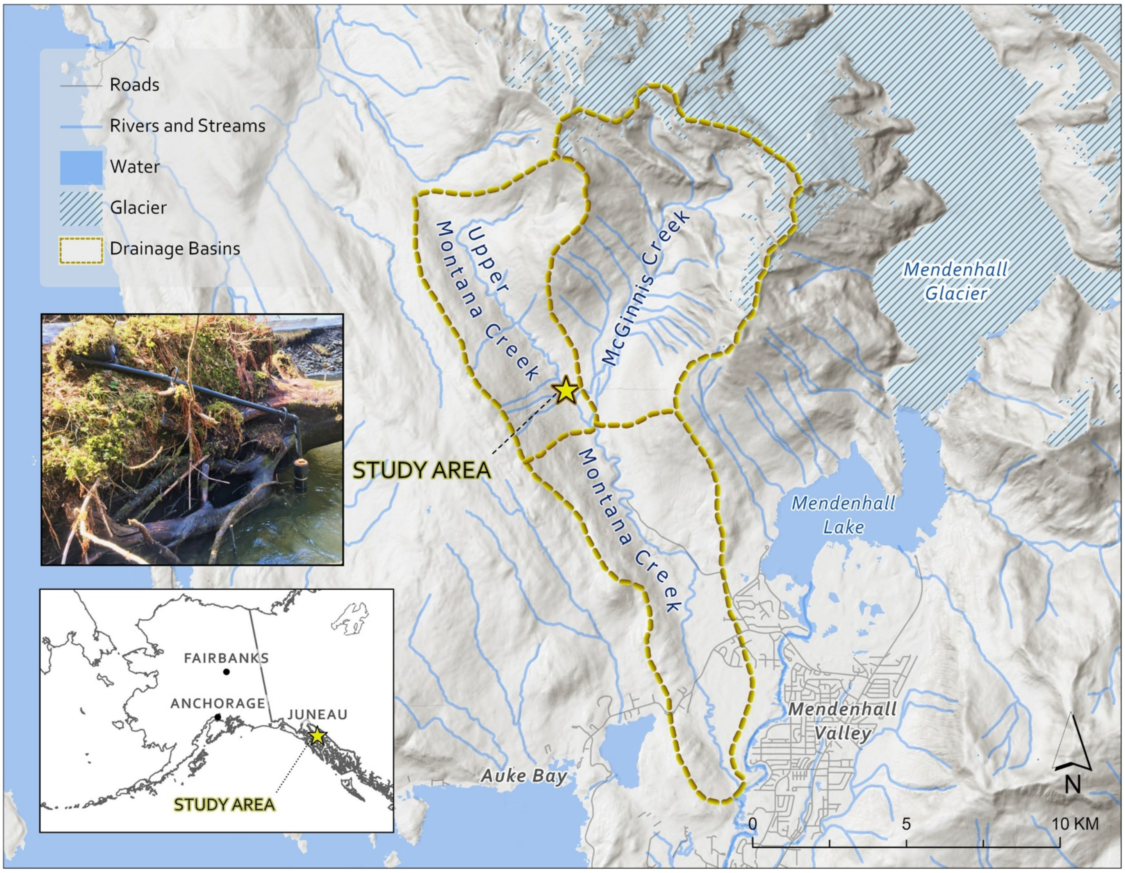

Figure 1. Map of the Kaxdigoowu Héen, also known as Montana Creek, study watershed located near Juneau, Alaska. The sampling location, indicated by the star, drains the 9.5 km^2 Upper Montana Creek watershed and is 20 km northwest of downtown Juneau. The sensor deployment at the site is shown in the picture on the map.

2. Methods

2.1. Study Site

The study site was the upper watershed of Kaxdigoowu Héen (Montana Creek), located in Southeast Alaska, near the city of Juneau (Alaska, USA). The Upper Kaxdigoowu Héen (Montana Creek) sub-basin has a watershed size of 9.5 km^2 and an average relief of 18° (Figure 1). Juneau experiences a maritime climate with a mean annual temperature of 5.6°C and precipitation averaging 170 cm each year (Palecki et al., 2021). Fluvial networks in Southeast Alaska have diverse sources of contributing water resulting in a broad watershed classification, including glacially fed, snow-fed, and predominantly rain-fed (Sergeant et al., 2020). Our study watershed has no measurable glacial coverage but seasonally accumulates an extensive snowpack in its upper hillslopes. Western hemlock (*Tsuga heterophylla*) and Sitka spruce (*Picea sitchensis*) mixed forest are the primary landcover (85%) followed by peat wetlands (7% landcover). The upper reaches of the watershed contain exposed bedrock with poorly developed soils, and sparse vegetation dominated by nitrogen-fixing alders (*Alnus* spp.). Kaxdigoowu Héen (Montana Creek) supports runs of four of the five species of Pacific Salmon (*Oncorhynchus keta, O. gorbuscha, O. tshawytscha*, and *O. kisutch*), as well as steelhead trout (*O. mykiss*), cutthroat trout (*O. clarkii clarkii*), Dolly Varden (*Salvelinus malma*), and sculpins (*Cottus spp*.).

2.2. Dissolved Organic Carbon and Alkalinity Sample Collection and Analysis

Surface water grab samples (n = 65) of DOC and alkalinity were collected at least once per week during dry periods and up to twice per day during storm events for the period of 24 April through 31 October 2021 (the main runoff season). Triplicate samples of DOC were filtered through a pre-combusted (450°C for 4 hr) glass fiber filter (0.7 μm) and collected in acid washed and pre-combusted (450°C for 4 hr) glass vials that were triple rinsed with filtered stream water. Upon return to the laboratory, the 40 mL DOC samples were acidified with 40 μL of 12 M hydrochloric acid and stored in the refrigerator for a maximum of 1 month before analysis. Dissolved organic carbon samples were analyzed on a Shimadzu TOC/TN-L-CSH by high temperature combustion, and concentrations were reported in mg C/L as the mean of 3–5 replicate injections. The standard deviation of the triplicate samples ranged from 0.011 to 1.0 mg/L with an average standard deviation of 0.134 mg/L.

Alkalinity samples were collected unfiltered from the stream in acid-washed polyethylene bottles ensuring there was no head space. Upon returning to the laboratory, samples were refrigerated and processed within 24 hr of collection. Alkalinity was measured as $CaCO_3$ (mg/L) via hydrochloric acid (0.02 N) titration to pH end points 4.4 and 4.7 (Method 2320 from the Standard Methods for the Examination of Water and Wastewater, 1999). Alkalinity concentrations were converted to mg C/L for direct comparison of carbon concentration to DOC under the assumption that the primary contributor to alkalinity in our system is bicarbonate (Cole et al., 2021). Triplicate stream water samples of δ^{13}C-DIC were filtered through a 0.2 μm nylon filter and collected in acid washed and pre-combusted (450°C for 4 hr) glass vials that were triple rinsed with filtered stream water. Vial caps were wrapped with parafilm and samples were stored in the refrigerator until sent to the University of Hawaii Analytical Lab for processing within 6 months of collection. One of the triplicate samples was run from each sampling event and two quality control (QC) samples were run alongside the submitted samples to verify accuracy and precision of isotope data.

2.3. Discharge Measurements

We installed a pressure transducer in PVC piping (In Situ Level TROLL 500, Fort Collins, Colorado, USA) that recorded measurements at 15-min intervals from the end of April (spring) through the first week of November (fall). Discrete measurements of discharge ($n = 20$) were made throughout the field season under a variable range of flow using a SonTek Flowtracker current meter (San Diego, California, USA). Concurrent stage and discrete discharge measurements were used to develop a rating curve, which was used to calculate discharge at 15-min intervals for the entire sampling period. These 15-min measurements were averaged to an hourly value. Pressure transducer measurements were interrupted 13 August to 14 August due to sensor displacement during the largest flow event of the season. To address this gap in our data, we estimated the missing discharge values using a regression equation developed between discharge at our site and at a National Weather Service stream gauge (NWS MCAA2) approximately 6 km downstream of the study reach that remained operational during the storm.

2.4. Sensor Data and Calculation of Daily Carbon Yields

A YSI Exo2 sonde (Yellow Springs, Ohio, USA) equipped with a wiper was deployed in the stream on 6 May 2021 and recorded hourly measurements of temperature (°C), turbidity (FNU), florescent dissolved organic matter (FDOM; QSU), and specific conductivity (μS/cm). The sensors were calibrated to known standards in the laboratory before installation. The conductivity sensor was calibrated using a 1,000 μS/cm standard for fresh water while the FDOM sensor was calibrated using a 300 QSU (100 RFU) quinine sulfate solution following YSI Exo sonde protocols. We downloaded the sensor data at least monthly over the summer and inspected the sensors for any debris or damage. At the time of download, we checked the sonde measurements against discrete measurements using a hand-held YSI ProDSS multi-probe (Yellow Springs, Ohio, USA) equipped with temperature, conductivity, and turbidity sensors and observed no deviation throughout the sampling period. At season end, we did a bucket test to affirm that the YSI ProDSS and YSI Exo sonde were performing consistently relative to one another.

Our site had relativity low turbidity for the entire sampling period, averaging 1.80 FNU, which is below the typical threshold where it is necessary to correct FDOM values for turbidity (Saraceno et al., 2009). However, turbidity exceeded 50 FNU during three storms and thus, we corrected our FDOM measurements for temperature and turbidity using an equation utilized for glacial and non-glacial streams (Boix Canadell et al., 2019). While site-specific corrections are considered preferable (Downing et al., 2012), it has also been shown that laboratory derived corrections for turbidity produce similar results for mid-to low-range turbidity measurements (<300 FNU), which applies to our study watershed (Saraceno et al., 2017). Linear regressions between DOC grab samples and corrected hourly FDOM measurements ($r^2 = 0.89$, $p < 0.001$) and alkalinity grab samples and hourly specific conductivity measurements ($r^2 = 0.94$, $p < 0.001$) were established to convert FDOM to DOC and specific conductivity to alkalinity. These relationships (Figure S1 in Supporting Information S1) were used to create an hourly time series of DOC and alkalinity concentrations for the sampling period.

2.5. Delineation of Individual Storms, and Metrics of Concentration-Discharge Relationships

Our method for storm delineation was adapted from Koch et al. (2021). Storms were defined as a doubling or more in flow from baseflow conditions to peak flow. The start of storm events was defined by the inflection point between baseflow conditions and the ascending limb, where discharge increased continuously between hourly measurements. Storm events ended either when flow conditions changed less than 0.01 m^3/s over the course of an hour or at the inflection point of the following storm. Storms with multiple peaks were divided into separate events if flow conditions dropped below 50% of the first peak between peaks. Storms were named by the first letter of the month in which they occurred and the storms' number order in the month (e.g., the first storm in May was M1; JN was used for June, and JU for July).

Concentrations of DOC and alkalinity were converted to a mass yield (kg C/km^2/h) by pairing hourly concentration and discharge measurements and normalizing for the watershed area (9.5 km^2). Discharge was converted from m^3/s to runoff in mm/h by normalizing hourly discharge measurements to the watershed area. To examine whether DOC and alkalinity were transport or source limited, we examined the b value in the power law relationship between hourly DOC/alkalinity yields and hourly runoff described by the equation: Flux = aQ^b, log transformed as log(Flux) = log(a) + b*log(Q), following Zarnetske et al. (2018). A power law b value of 1 indicates chemostasis, >1 indicates transport limitation, and <1 indicates source limitation (Zarnetske et al., 2018). The power law relationship and b value were estimated using the hourly time series of DOC and alkalinity and discharge for the entire study period and for each individual storm event.

To calculate a hysteresis index (HI), each storm was normalized for discharge and DOC or alkalinity concentration (Lloyd et al., 2016b). Hourly discharge and DOC/alkalinity measurements for each storm were normalized by subtracting the minimum observed value of discharge and DOC/alkalinity, then dividing by the maximum minus the minimum values observed during the storm event, resulting in unitless values of flow and C ranging from 0 to 1 (following Lloyd et al., 2016b). Linear interpolation was used to calculate the normalized values of DOC or alkalinity at 25%, 50%, and 75% intervals of normalized flow and the difference in concentration between the rising and the falling limb at each of those intervals was calculated; values were averaged to generate a HI for each storm.

3. Results

3.1. Discharge Over the Sampling Period

Across the sampling period, hourly streamflow averaged 1.10 m^3/s and ranged from 0.14 to 24.69 m^3/s with both the highest and lowest flows occurring in August (Figure 2). Early season flows were influenced by snow melt and rain events. Hourly streamflow oscillated sub-daily as warm daytime air temperatures melted snow in the catchment, a diurnal pattern that lasted through the first week of June. July through early August was generally a very dry period, with the lowest flows of the sampling period interspersed with rain-driven flow events. Starting the second week of August, streamflow was driven by more frequent rain events. As air temperatures dropped in October, snow accumulated in the higher elevations in the catchment and discharge became less responsive to precipitation. Over the sampling period, we measured CQ relationships for 23 storms.

3.2. Streamwater Dissolved Organic Carbon and Alkalinity Concentrations

Streamwater concentrations of DOC averaged 3.29 mg C/L and ranged from 0.54 to 10.81 mg C/L across the study period (Figure 2a). The lowest DOC concentrations coincided with low flows in June and July, and the highest concentrations occurred in the first two flow events in August. Concentrations of alkalinity averaged 2.33 mg C/L and ranged from 0.53 to 4.20 mg C/L (Figure 2b). Low alkalinity concentrations generally occurred during high flow events, with the lowest concentrations occurring in May (Figure 2b). There were occasional peaks in DOC concentration and drops in alkalinity that co-occurred during precipitation events (as reported by local NOAA weather station PAJN) that did not cause a measurable change in flows for either our pressure transducer or the downstream NWS gauge.

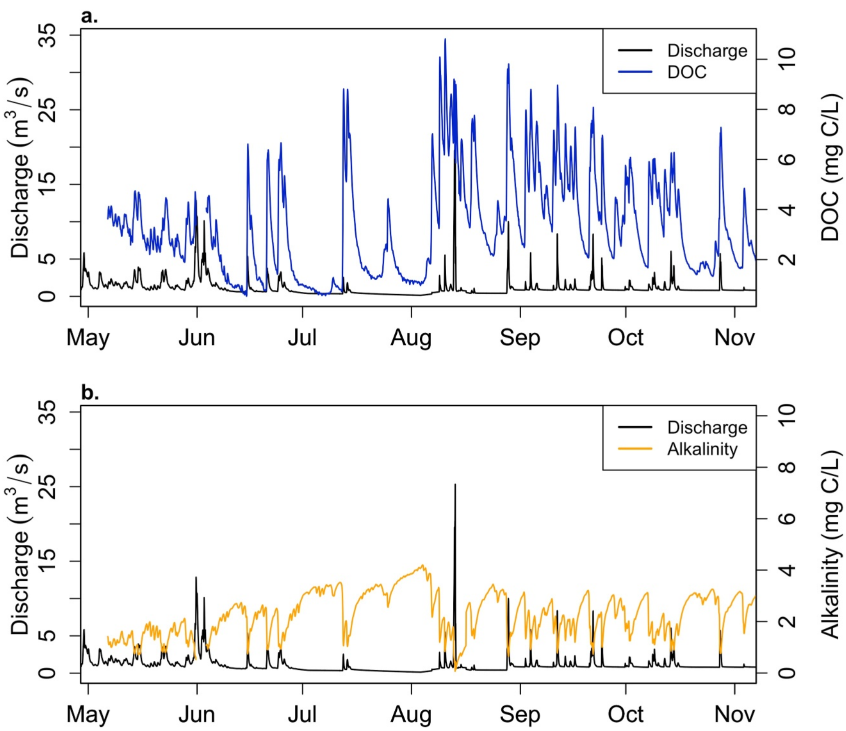

Figure 2. Hourly streamflow (m^3/s) and concentrations of (a) dissolved organic carbon (DOC) and (b) alkalinity (mg C/L) in Kaxdigoowu Héen (Montana Creek), Alaska for the May through November 2021 sampling period.

Concentrations of DOC typically were elevated during periods of high flow over the entire study period (Figures 3 and 4a). However, this relationship varied with DOC concentrations of <4.0 mg C/L observed in May and June, but spanned concentrations of <1.0 mg C/L to >10.0 mg C/L later in the summer and early autumn (Figure 5). In contrast, alkalinity concentrations exhibited a non-linear decrease as discharge increased over the study period (Figures 3 and 4b). Alkalinity concentrations did not surpass 2.0 mg C/L until July and peaked at 4.2 mg C/L in early August but did not exceed 4 mg C/L for the remainder of the sampling period. Values for δ^{13}C-DIC ranged from −5.0 to −11.6‰ with a mean of −6.8‰ (Figure S2 in Supporting Information S1). Although δ^{13}C-DIC values did not show a strong seasonal pattern across the study period, values showed a mild, negative correlation with discharge (r^2 = 0.17, p = 0.04) and were generally the most depleted during periods of high flow (particularly during the large storm in August). This is consistent with the flushing of alkalinity that is derived mainly from biogenic sources in adjacent terrestrial ecosystems (Duvert et al., 2019).

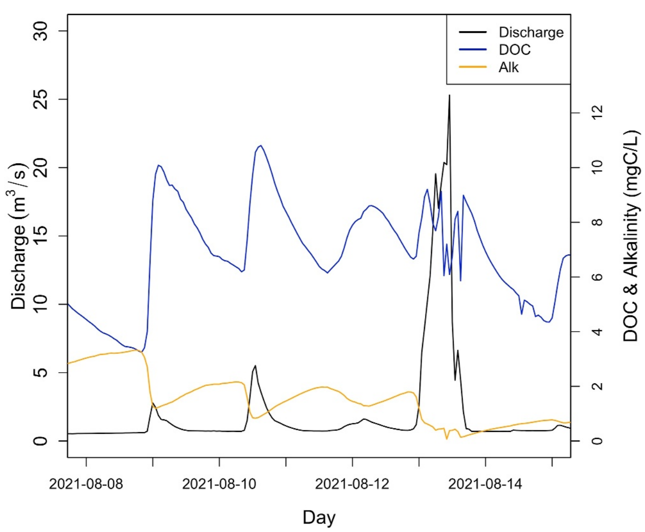

Figure 3. Hourly streamflow (m^3/s) and concentrations of dissolved organic carbon (DOC) and alkalinity (Alk) (mg C/L) in Kaxdigoowu Héen (Montana Creek) during the first four storms in August (A1–A4), A4 was the storm with the highest flows during our sampling period.

The relationship between DOC and discharge was more linear (r^2 = 0.75) and constrained in May (Figure 5a), which had both the smallest range of DOC concentrations and measured discharge, compared to other months. Discharge and DOC also had a strong linear fit in June, (r^2 = 0.76; Figure 5b); however, data points were more scattered in July resulting in a weaker linear fit (r^2 = 0.42; Figure 5c). The widest range of flow conditions and DOC concentrations were measured in August (Figure 5d), which resulted in a more complex CQ pattern than other months. Specifically, the August CQ relationship became more asymptotic than linear, with sharp decreases in concentration that occurred at varying stages of flow. This pattern transitioned into September and October (Figures 5e and 5f), when an asymptotic relationship remained but concentrations of DOC dropped at similar discharge values, resulting in a more consistent asymptotic pattern relative to

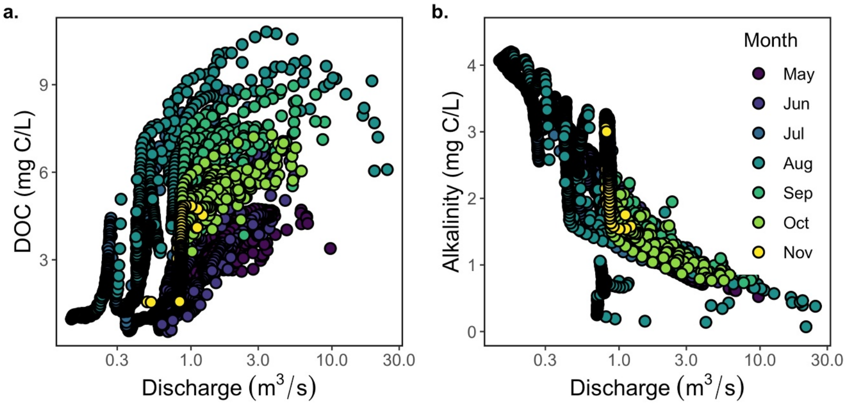

Figure 4. Hourly concentration data (mg C/L) for (a) dissolved organic carbon (DOC) and (b) alkalinity versus discharge (m^3/s) in Kaxdigoowu Héen (Montana Creek), Alaska across the entire study period. The discharge measurements have been log transformed but values on the *x*-axis represent discharge in m^3/s for ease of interpretation. Every other *x*-axis tick represents a ten-fold increase in discharge. Data points are colored by date.

August. There was also a decreased range of DOC concentrations under comparable flow conditions from September (Figure 5e) into October (Figure 5f).

Similar to DOC, alkalinity had the strongest linear relationship in May ($r^2 = 0.66$) and June ($r^2 = 0.78$) (Figures 6a and 6b). Progressing from June to August, the range of flow conditions and alkalinity concentrations broadened (Figures 6c and 6d). The CQ relationship become more asymptotic in July and August. The pattern of elevated concentrations at low flows and asymptotic behavior with decreasing concentrations at higher flows became more consistent in September (Figure 6e) and October (Figure 6f).

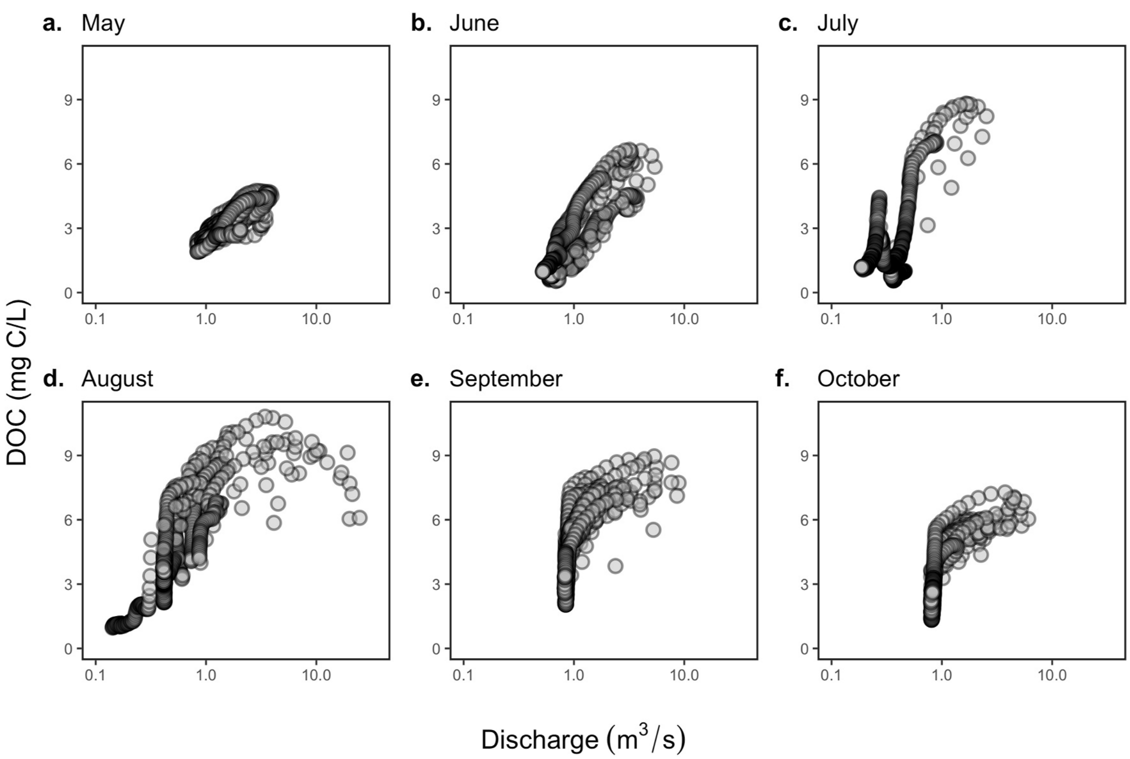

Figure 5. Hourly dissolved organic carbon (DOC) concentration (mg C/L) versus discharge (m^3/s; log scale) in Kaxdigoowu Héen (Montana Creek), Alaska separated by month.

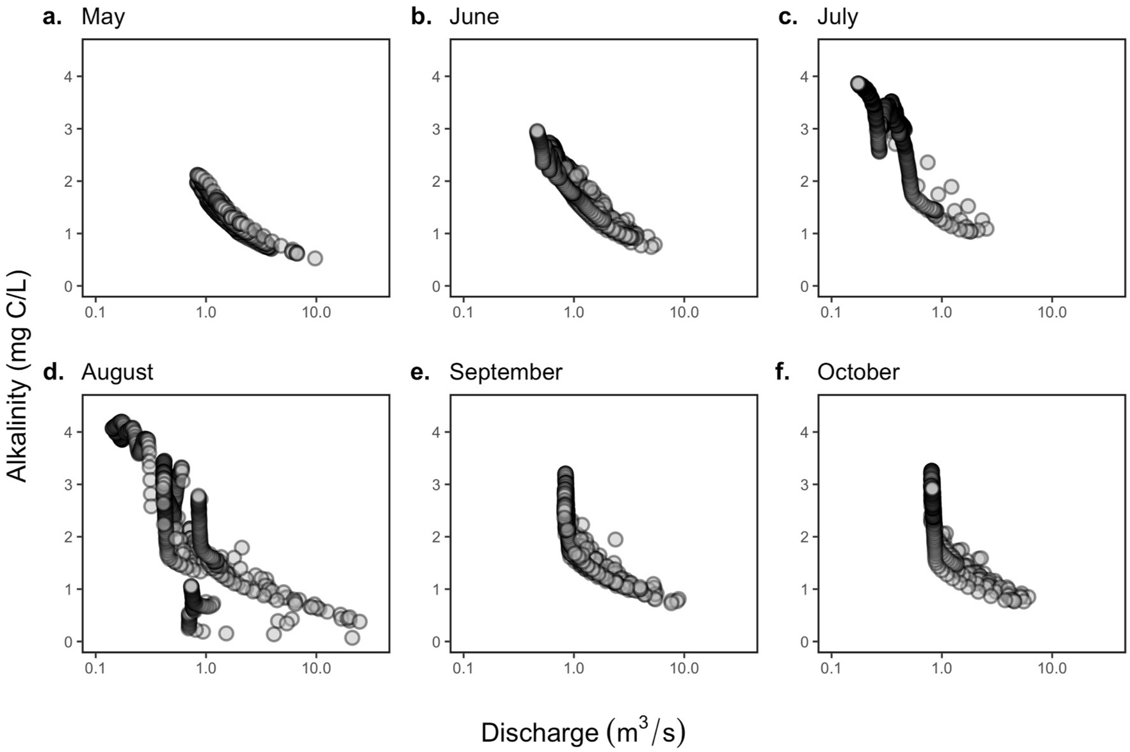

Figure 6. Hourly alkalinity concentration (mg C/L) versus discharge (m^3/s; log scale) in Kaxdigoowu Héen (Montana Creek), Alaska separated by month.

3.3. *b* Values for the Sampling Period

Across the sampling period, the average *b* values for the power law model between runoff versus DOC and alkalinity yields were 1.58 and 0.48, respectively (Figure 7). The overall fit for the sampling period was similar to the relationships for individual storms (Table 1). For DOC, the *b* value was greater than one for every storm (mean $b = 1.42$), except for the fourth storm in August (A4, Table 1), when the *b* value was just below one ($b = 0.99$). For alkalinity, *b* values for most storms were less than one, with a mean *b* value for all of storms equal to 0.50, which is in line with the *b* value for the entire sampling period. For alkalinity, A4 was the highest flow event of the sampling period and the only storm with a *b* value above 1 ($b = 1.02$).

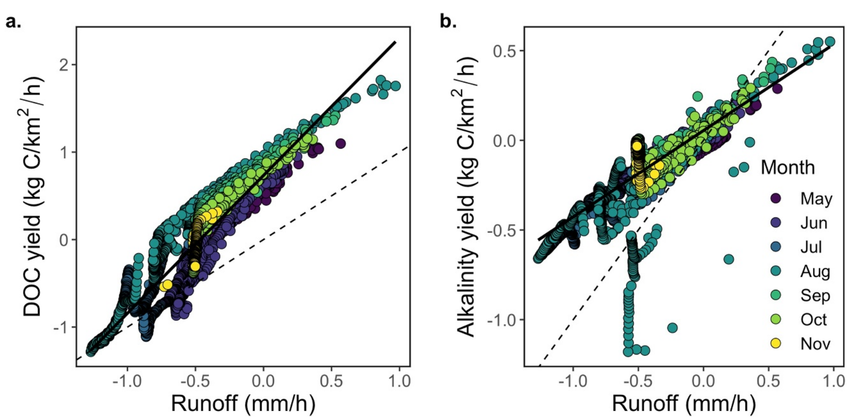

Figure 7. Power law relationship (solid line) between yields (kg/km^2/h) of (a) dissolved organic carbon (DOC; $y = 0.73 + 1.58x$, $r^2 = 0.81$, $p < 0.001$) and (b) alkalinity ($y = 0.05 + 0.48x$, $r^2 = 0.65$, $p < 0.001$) and mm/h of runoff in Kaxdigoowu Héen (Montana Creek), Alaska. Dashed line follows a one-to-one slope.

Table 1
Measured Indices for Each Storm Include Starting Date and Maximum Flow and for Dissolved Organic Carbon (DOC) and Alkalinity, Include the b Value for the Power Law Relationship for an Individual Storm and r^2 for the Fit of the Line and Hysteresis Index (HI) on a Scale From −1 to 1, With Negative Numbers Indicating Counterclockwise Hysteresis and Positive Numbers Indicating Clockwise Hysteresis

Storm	Date start	Max flow (cms)	DOC *b* (r^2)	Alkalinity *b* (r^2)	DOC HI	Alkalinity HI
M1	5/13/21	3.93	1.426 (0.99)	0.333 (0.95)	0.002	0.273
M2	5/20/21	4.47	1.397(0.96)	0.351 (0.96)	−0.439	0.065
JN1	6/15/21	5.40	1.654 (0.86)	0.472 (0.90)	−0.451	0.247
JN2	6/20/21	3.68	1.673 (0.87)	0.455 (0.90)	−0.451	0.225
JN3	6/23/21	3.29	1.763 (0.95)	0.447 (0.93)	−0.337	0.202
JU1	7/12/21	2.54	1.769 (0.79)	0.538 (0.77)	−0.398	0.265
JU2	7/13/21	1.84	1.613 (0.95)	0.401 (0.75)	−0.253	0.206
A1	8/8/21	2.81	1.514 (0.81)	0.437 (0.47)	−0.584	0.384
A2	8/10/21	5.44	1.219 (0.98)	0.582 (0.94)	−0.491	0.224
A3	8/11/21	1.61	1.379 (0.97)	0.465 (0.87)	−0.361	0.199
A4	8/12/21	24.69	0.992 (0.99)	1.020 (0.76)	0.515	0.131
A5	8/27/21	10.17	1.298 (0.98)	0.538 (0.95)	−0.091	0.141
S1	9/3/21	5.62	1.286(0.96)	0.507 (0.79)	−0.316	0.150
S2	9/11/21	8.89	1.470 (0.98)	0.558 (0.96)	−0.333	0.122
S3	9/13/21	2.21	1.248 (0.94)	0.450 (0.74)	−0.403	0.259
S4	9/14/21	1.61	1.457 (0.95)	0.453 (0.77)	−0.677	0.480
S5	9/15/21	2.36	1.554 (0.94)	0.386 (0.67)	−0.355	0.226
S6	9/20/21	8.60	1.376 (0.94)	0.491 (0.84)	−0.117	0.049
S7	9/23/21	5.25	1.302 (0.94)	0.545 (0.85)	−0.686	0.482
O1	10/1/21	2.14	1.330 (0.96)	0.484 (0.82)	−0.566	0.481
O2	10/7/21	3.10	1.421 (0.88)	0.490 (0.86)	−0.403	0.293
O3	10/13/21	6.07	1.267 (0.99)	0.550 (0.96)	−0.224	0.095
O4	10/27/21	5.53	1.230 (0.97)	0.517 (0.86)	−0.497	0.273

Note. Storms were delineated by their month (first letter of the month in which they occurred; JN for June and JU for July) and number order within that month.

3.4. Slope Coefficients (*b* Values) and Hysteresis Metrics for Individual Storms

The *b* value for alkalinity and DOC and starting dates for each storm were significantly correlated. For DOC, this relationship was negative ($r^2 = 0.24$, $p = 0.02$; Figure 8a), with the *b* value for storms decreasing from May to November but still demonstrating transport limitation. Alkalinity showed a non-significant positive trend between the date and *b* value for each storm ($r^2 = 0.07$, $p = 0.21$; Figure 8b), with the *b* value increasing over the sampling period but still demonstrating source limitation. The first two storms of the season (M1 and M2) were rain on seasonally accumulated snowpack events that weighted the linear model fit for both alkalinity and DOC (Figures 8a and 8b). Removing those two outliers from the regression, on the basis of their hydrologic dissimilarity from the rest of the year's storms, resulted in a better fit for DOC ($r^2 = 0.40$, $p = 0.002$; Figure 8a). For alkalinity, with M1 and M2 removed there was not a significant relationship between storm timing and the *b* value for each storm ($r^2 = 0.003$, $p = 0.83$; Figure 8b). Similarly, the fourth storm in August (A4) drove DOC and alkalinity toward chemostasis.

The hysteresis index for DOC was typically negative and characterized by counterclockwise hysteresis during storms across the study period (mean HI = −0.34; Table 1). There were two instances, the first storm in May (M1) and fourth storm in August (A4), when DOC did not follow this trend, but rather showed clockwise hysteresis. Alkalinity consistently had a positive HI, demonstrating clockwise hysteresis (mean HI = 0.24). For a few storm sequences, when storms followed in close succession (within 2 or 3 days of one another), the HI for both alkalinity

10.1029/2025JG009090

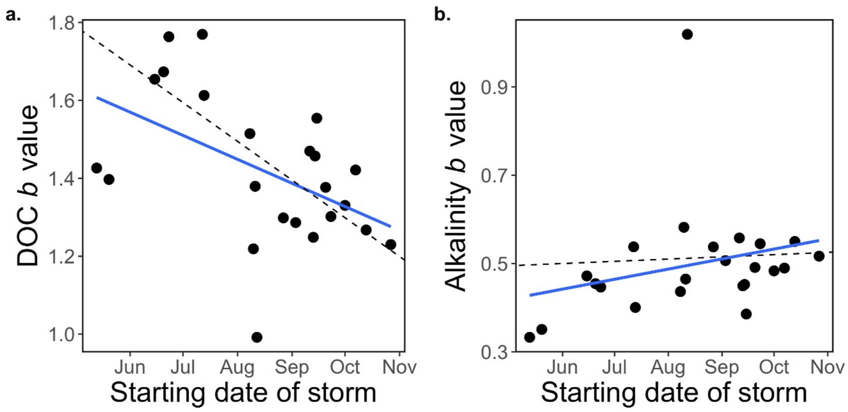

Figure 8. Slope coefficients (*b* values) for individual storms over the sampling period for (a) dissolved organic carbon (DOC) and (b) alkalinity in Kaxdigoowu Héen (Montana Creek), Alaska. The blue line represents the linear fit for all of the storms (DOC: $y = 38.850–0.002x$, $r^2 = 0.24$, $p = 0.02$; Alkalinity: $y = -13.52 + 0.0007x$, $r^2 = 0.07$, $p = 0.21$). The dotted line represents the linear fit excluding M1 and M2, which were both rain on snow events in early May (DOC: $y = 62.035–0.003x$, $r^2 = 0.40$, $p = 0.002$; Alkalinity: $y = -2.583 + 0.0001x$, $r^2 = 0.003$, $p = 0.83$).

and DOC moved closer to zero with each subsequent storm. For example, in the first three storms in August (A1–A3; Table 1), the widest range of DOC concentrations between the ascending and descending limb was observed during the first storm (A1). For the following storm (A2), the range of DOC concentrations was narrow and did not return to the level at which the first storm started (Figure 9a). For the same set of storms in August, alkalinity also had a HI that moved toward zero; however, this was because alkalinity concentrations were not rebounding to the highest concentration of the first storm, with each subsequent flow event (Figure 9b). This pattern was seen in the following sets of storms: JN2 and JN3, JU1 and JU2, and A1 through A4. Overall, HI values for DOC generally decreased across the study period, while values for alkalinity increased (Table 1). This seasonal pattern resulted in a negative correlation between HI values for DOC and alkalinity ($r^2 = 0.36$, $p < 0.01$).

4. Discussion

We found contrasting seasonal and storm event-driven variation in the relationship between dissolved carbon concentrations and discharge. Concentrations of DOC and alkalinity showed contrasting responses to discharge, as DOC concentrations increased and alkalinity decreased with increasing streamflow (Figures 2 and 3). The negative relationship between HI values and carbon species further supports the notion that DOC and alkalinity have different sources and transport pathways in our study watershed. The relationship between discharge and concentrations of DOC and alkalinity can be variable and dependent on several factors including land-cover,

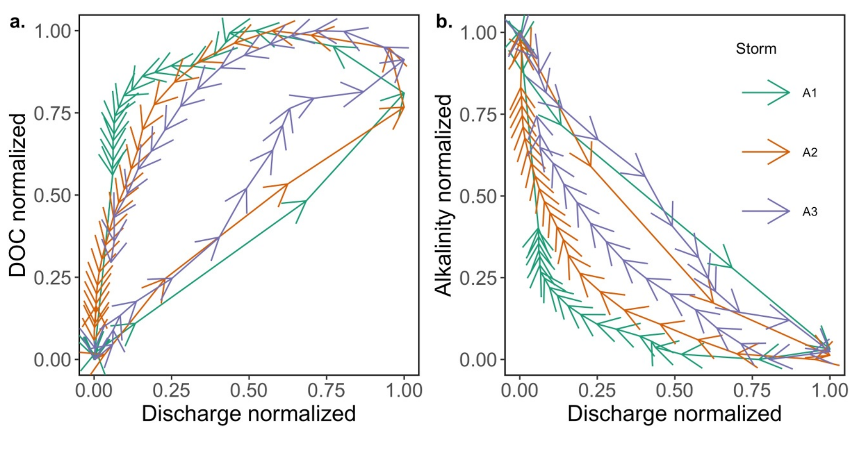

Figure 9. Normalized hysteresis plots of storms for the first three storms in August (A1, A2, and A3) in Kaxdigoowu Héen (Montana Creek), Alaska for (a) dissolved organic carbon (DOC) and (b) alkalinity. Each arrow represents an hourly measurement and arrows point in the direction of the passage of time.

underlying geology, season, and hydrology (Chaplot & Mutema, 2021; Jantze et al., 2015; Leach et al., 2016; Perdrial et al., 2014). However, similar patterns in CQ for DOC and alkalinity have been found in other high latitude watersheds (Koch et al., 2021). For both DOC and alkalinity, the relationship shifted from a more constrained and linear relationship in the spring to a broader and non-linear pattern in July and August, then a more repetitive and asymptotic pattern during the autumn rainy season (Figures 5 and 6). Our results provide evidence that antecedent flow conditions (i.e., storms in close succession) impacted the concentration of DOC and alkalinity in storms that followed (Figure 9, Table 1), with DOC and alkalinity concentrations starting from a higher or lower baseline, respectively, when storms follow in close succession. Elucidating the interactions between season, antecedent conditions, and CQ relationships for multiple forms of carbon will become more important to watershed carbon budgets as hydrologic extremes become more common (McMillan et al., 2018).

4.1. Seasonal Changes in Dissolved Organic Carbon and Alkalinity Sources and Flowpath

Seasonal shifts in CQ relationships likely result from differing flowpaths and sources of DOC (Sanderman et al., 2009) and alkalinity (Campeau et al., 2017) within the study watershed, with flowpaths strongly influencing how different sources of DOC and DIC are mobilized to streams and processed before reaching surface waters (Douglas et al., 2013; Johnson et al., 2011; Wen et al., 2022). In the spring, snowmelt-driven flushing of DOC from saturated soils (Boyer et al., 1997) likely contributed to the initially linear and constrained relationship we observed between flow and DOC (Figures 5a and 5b). A buildup of DOC in soil waters from heterotrophic breakdown of soil carbon is thought to be the main contributor of DOC during winter and spring months (Brooks et al., 1999). The mid-summer months coincide with the broadest range of flow conditions and DOC concentrations (Figures 5c and 5d). Low flow periods in June through August are dominated by groundwater inputs to streamwater and thus can be low in DOC, likely due to microbial processing of DOC and mineral sorption along soil flowpaths (Kaiser & Kalbitz, 2012). In contrast, rain events during this period can mobilize pools of high concentration DOC, connecting watershed sources (organic rich soil horizons, stemflow, and throughfall) to surface waters (Behnke et al., 2022) via shallow sub-subsurface flowpaths. From mid-August through October, decomposition and leaf senescence likely contribute to the DOC pool (Singh et al., 2014). Hydrologic connectivity within the watershed is also high during the late summer/fall wet season due to frequent rain events, and dilution from storm events may contribute to our observed reduced DOC concentrations, negative trend in *b* values, and overall decrease in HI values (Figures 5e and 5f, Table 1).

While DOC is primarily biologically sourced and transported to surface water via shallow subsurface flowpaths, alkalinity in the study watershed appears to have a primarily geologic source (mean: δ^{13}C-DIC = −6.8‰, Figure S2 in Supporting Information S1, Campeau et al., 2017). Previous research has shown that corresponding increases in DIC concentration and an enrichment in δ^{13}C-DIC values are indicative of zones of groundwater input to surface water (Doctor et al., 2008; Duvert et al., 2018, 2019). These studies support our hypothesis that alkalinity is derived mainly from geologic sources in our study watershed, particularly during periods of low flow when groundwater inputs to surface flow are likely the highest. Low concentrations of alkalinity in May are likely related to frozen and/or saturated soils and the predominance of shallow near-surface flowpaths that do not allow for sufficient contact time with underlying bedrock. This contrasts with studies that have found that inorganic carbon can build up in the snowpack, leading to higher concentrations at the onset of snowmelt (Dinsmore et al., 2011; Sakamoto et al., 1999), which were not observed in our study. Higher concentrations in June through August are likely related to undiluted (i.e., by rainwater) groundwater flowpaths and temperatures that increase rock weathering (Gaillardet et al., 2019) and production of CO_2 instream and in soils (Li et al., 2010). Given that alkalinity is likely predominantly geologically derived in our watershed and is delivered to surface waters during periods of low flow when high groundwater inflow rates are likely highest, reduced concentrations in September and October may be related to reduced temperatures limiting alkalinity production. Lower alkalinity could also be attributed to the frequent flushing of shallow subsurface flowpaths that interact less with bedrock compared to groundwater flowpaths.

4.2. Trends in Power Law Functions (*b* Values) Between Runoff and Carbon Yields

The overall and individual storm *b* values reflect differences in source and mobilization of DOC and alkalinity. For DOC, the overall *b* value was >1 and indicates transport limitation within the watershed across the study period. The presence of watershed wetland coverage has been shown to be associated with transport limitation for DOC (Zarnetske et al., 2018). Given the wetland coverage of 7%, expansive forest, and carbon rich soils in the watershed (D'Amore et al., 2015), we expected to see transport limitation for DOC. However, alkalinity was strongly source limited (b value < 1), which corroborates that groundwater was likely the primary source for alkalinity (Duvert et al., 2018).

Seasonal trends in the b values for individual storms suggested that DOC over our sampling period became less transport limited as the b value shifted from a peak of 1.76 (JU2 $r^2 = 0.79$) in June and July toward 1.23 (O4 $r^2 = 0.97$) in October (Table 1). Removing the two early season rain on snow events that were hydrologically dissimilar from the rest of the year further strengthens the observed pattern of decreasing transport limitation across the study period. The June and July high b values could be related to ample DOC production in soils and infrequent storms that deliver abundant DOC to streamwater but at the same time, do not exhaust terrestrial source pools. However, in September and October, mobilization of DOC from frequent storm events in a more hydrologically connected watershed, could lead to a b value closer to one. This suggests that under increasingly wet hydrologic conditions, the export of DOC switches from transport to source limitation.

For individual storms, alkalinity b values were below one except during the largest storm of the season that occurred in mid-August (A4), indicating source limitation over the sampling period (Table 1). The trend in b values was positive over the sampling period but removing the two early season rain-on-snow events resulted in a non-significant relationship between storm date and alkalinity b values (Figure 8b). The lack of seasonal relationships supports the hypothesis that alkalinity production is primarily through rock weathering reactions, this contrasts with other watersheds where inorganic carbon is primarily produced by seasonally influenced biological processes (e.g., soil mineralization, root respiration; Campeau et al., 2019).

4.3. Individual Storms and Inter-Storm Dynamics

Hysteresis patterns and b values indicated that relationships between flow and concentrations differed over the sampling period. Other studies have found similar overall hysteresis directions and b values for DOC and DIC for individual storms (Koch et al., 2021; Li et al., 2022). For DOC, CCW hysteresis indicates mobilization of more distal or slower to mobilize (e.g., wetland) sources of DOC reaching surface waters later in the storm. For alkalinity, CW hysteresis indicates a dilution of proximate sources. Given that HI values and direction showed no correlation with the time of year, we expect that the primary location of these sources of DOC or alkalinity are not changing seasonally. Wetland landcover is typically associated with CCW hysteresis for DOC, as observed in the study watershed, although HI values for DOC have been shown to vary depending on other factors including land cover, wetland location, and season (Ducharme et al., 2021; Finlay et al., 2006; Vaughan et al., 2017). For DOC, the HI switched direction to CW twice over the study period (Table 1). The first storm in the spring (M1) had CW hysteresis, potentially related to the existing snowpack, frozen soils and predominance of near surface flowpaths. The largest storm in August (A4) also had a switch in HI direction and the lowest b value for DOC (Table 1). This indicates that during this high flow event, DOC switched from transport limitation to chemostasis when DOC production and mobilization matched runoff as the event progressed.

There was some evidence that antecedent conditions influenced hysteresis in DOC and alkalinity concentrations (Figure 9). During June through August when a series of storms followed within 1–2 days of each other (Table 1; JN2–JN3, JU1–JU2), the HI values for DOC and alkalinity approached zero with each subsequent storm, and in one instance (Table 1; A1–A4), switched direction. This storm series shrinking hysteresis loop pattern has also been noted for nitrate concentrations in an agriculturally influenced watershed (Lloyd et al., 2016a). Only three sets of storms exhibited this kind of pattern over our 6-month sampling window, indicating that longer-term monitoring would be needed to determine the significance of this pattern to watershed carbon dynamics. However, this does suggest that there is inter-storm connection of distal pools of high concentration DOC and inter-storm dilution of alkalinity sources with frequent storms. Additionally, with DOC we found that there is the potential to dilute source pools if a large storm occurs during high flow sequences (Table 1, A1–A4). In that same storm series, alkalinity switched from source limited to chemostatic (Table 1, A1–A4), indicating mobilization of alkalinity sources that may not typically reach surface waters.

Storm events are significant in that they can export large quantities of DOC and DIC to downstream ecosystems (Dalzell et al., 2007; Raymond & Saiers, 2010). Our findings suggest that storms in close succession have the potential to deplete or dilute sources of DOC and mobilize disconnected sources of alkalinity. Therefore, any storm's impact on dissolved carbon export could be impacted by antecedent conditions within the watershed, including time of year and previous flow conditions. This corroborates other findings that show antecedent conditions such as soil moisture, wildfire history, prolonged drought, and freeze-thaw cycles can alter CQ relationships (Biron et al., 1999; McMillan et al., 2018).

5. Conclusion

Our findings suggest that shifts in hydroclimate will likely impact DOC and alkalinity CQ relationships, altering the timing and magnitude of carbon export from coastal watersheds in Southeast Alaska. Predicted increases in the frequency and intensity of storm events in the region (Lader et al., 2020, 2022) will likely impact concentrations of DOC and alkalinity in surface waters, with larger storms having the potential to deplete DOC sources depending on seasonal timing and antecedent conditions. Alternatively, prolonged dry periods in the summer may lead to groundwater-driven flows with low DOC concentrations and high alkalinity. In this scenario, alkalinity would have a proportionately larger contribution to watershed carbon export during these dry periods (Delbecq et al., 2024). Storms that do occur during these dry periods may readily mobilize high concentrations of DOC. We expect that interannual variability in weather patterns (i.e., dry vs. wet years) will alter the production and mobilization of DOC and alkalinity. Because these different forms of carbon have different processes that regulate their production and mobilization into surface waters, we would expect that biological sources of DOC will be more altered by changes in hydroclimate in the region compared to inorganic carbon. A better understanding of streamwater carbon export during the winter months will become more important because increasingly frequent rain on snow events (Musselman et al., 2018) may have different CQ relationships for DOC and alkalinity that are poorly explained by data collected from spring through autumn.

Overall, our findings show that high resolution quantification of CQ relationships can further our understanding of seasonal patterns and watershed-scale controls on dissolved carbon export from forested watersheds. Establishing a baseline understanding of event-scale and seasonal changes in CQ relationships can help watershed scientists monitor how carbon CQ relationships are changing with year-to-year variation in hydrology and over the longer term. This baseline understanding may also reveal how watershed biogeochemical and ecological processes are altered by climate change (Schlesinger & Bernhardt, 2020) and land use (Han Lu et al., 2014; Yamashita et al., 2011). As extreme storms and periods of drought become more common, understanding how altered flow conditions interact with the production and mobilization of dissolved carbon will improve our understanding of the impact of hydroclimate shifts on watershed carbon cycling (Leach et al., 2016).

Acknowledgments
This work was completed as partial fulfillment of a Master of Science degree in Fisheries at the University of Alaska Fairbanks and was funded by the U.S. Geological Survey (USGS) Alaska Climate Adaptation Science Center in partnership with the USGS Pacific Island Climate Adaptation Science Center. We also received support to fund undergraduate researchers from the University of Alaska Southeast through Alaska EPSCOR Grant OIA-1753748, NSF ORE-CZ EAR-2227821, and NSF Grant 1557186. We thank the U.S. Forest Service Pacific Northwest Research Station for their in-kind support of laboratory space and personnel time. We thank our collaborators Tracy Wiegner, Steven Colbert, and Walter Boger from the University of Hawai'i (UH) Hilo as well as the UH Hilo Analytical Lab. Staff from the Alaska Coastal Rainforest Center, the University of Alaska Fairbanks College of Fisheries and Ocean Sciences, and the Alaska Cooperative Fish and Wildlife Research Unit for the smooth administration of this project. University of Alaska Southeast undergraduate students, Lucy Franklin, Ezra Grey, John Seymour, Randy Brannan, and Naomi Boyles-Muehleck for field data collection and sample processing. We thank Ed Neal, Alaska Hydroscience, for developing the rating curve for our flow data and Josh Paul for Figure 1. This work took place on the traditional lands of the Aak'w Kwáan Tlingit. Any use of trade, firm, or product names is for descriptive purposes only and does not imply endorsement by the U.S. Government.

Conflict of Interest

The authors declare no conflicts of interest relevant to this study.

Data Availability Statement

All data in this study are available online (https://doi.org/10.5066/P13JEBFP) through ScienceBase.

References

Aufdenkampe, A. K., Mayorga, E., Raymond, P. A., Melack, J. M., Doney, S. C., Alin, S. R., et al. (2011). Riverine coupling of biogeochemical cycles between land, oceans, and atmosphere. *Frontiers in Ecology and the Environment*, *9*(1), 53–60. https://doi.org/10.1890/100014

Behnke, M. I., Fellman, J. B., D'Amore, D. V., Gomez, S. M., & Spencer, R. G. M. (2022). From canopy to consumer: What makes and modifies terrestrial DOM in a temperate forest. *Biogeochemistry*, *164*(1), 185–205. https://doi.org/10.1007/s10533-022-00906-y

Bidlack, A. L., Bisbing, S. M., Buma, B. J., Fellman, J. B., Floyd, W. C., Giesbrecht, I., et al. (2021). Climate-mediated changes to linked terrestrial and marine ecosystems across the Northeast Pacific coastal temperate rainforest margin. *BioScience*, *71*(6), 581–595. https://doi.org/10.1093/biosci/biaa171

Biron, P. M., Roy, A. G., Courschesne, F., Hendershot, W. H., Côté, B., & Fyles, J. (1999). The effects of antecedent moisture conditions on the relationship of hydrology to hydrochemistry in a small forested watershed. *Hydrological Processes*, *13*(11), 1541–1555. https://doi.org/10.1002/(sici)1099-1085(19990815)13:11<1541::aid-hyp832>3.0.co;2-j

Boix Canadell, M., Escoffier, N., Ulseth, A. J., Lane, S. N., & Battin, T. J. (2019). Alpine glacier shrinkage drives shift in dissolved organic carbon export from quasi-chemostasis to transport limitation. *Geophysical Research Letters*, *46*(15), 8872–8881. https://doi.org/10.1029/2019GL083424

Boyer, E. W., Hornberger, G. M., Bencala, K. E., & McKnight, D. M. (1997). Response characteristics of DOC flushing in an alpine catchment. *Hydrological Processes*, *11*(12), 1635–1647. https://doi.org/10.1002/(sici)1099-1085(19971015)11:12<1635::aid-hyp494>3.0.co;2-h

Brooks, P. D., McKnight, D. M., & Bencala, K. E. (1999). The relationship between soil heterotrophic activity, soil dissolved organic carbon (DOC) leachate, and catchment-scale DOC export in headwater catchments. *Water Resources Research*, *35*(6), 1895–1902. https://doi.org/10.1029/1998WR900125

Campeau, A., Bishop, K., Amvrosiadi, N., Billett, M. F., Garnett, M. H., Laudon, H., et al. (2019). Current forest carbon fixation fuels stream CO_2 emissions. *Nature Communications*, *10*(1), 1876. https://doi.org/10.1038/s41467-019-09922-3

Campeau, A., Wallin, M. B., Giesler, R., Löfgren, S., Mörth, C. M., Schiff, S., et al. (2017). Multiple sources and sinks of dissolved inorganic carbon across Swedish streams, refocusing the lens of stable C isotopes. *Scientific Reports*, *7*(1), 9158. https://doi.org/10.1038/s41598-017-09049-9

Chaplot, V., & Mutema, M. (2021). Sources and main controls of dissolved organic and inorganic carbon in river basins: A worldwide meta-analysis. *Journal of Hydrology*, *603*, 126941. https://doi.org/10.1016/j.jhydrol.2021.126941

Cole, J. J., Hararuk, O., & Solomon, C. T. (2021). The carbon cycle: With a brief introduction to global biogeochemistry. In *Fundamentals of ecosystem science* (2nd ed., pp. 131–160). Elsevier.

Dalzell, B. J., Filley, T. R., & Harbor, J. M. (2007). The role of hydrology in annual organic carbon loads and terrestrial organic matter export from a midwestern agricultural watershed. *Geochimica et Cosmochimica Acta*, *71*(6), 1448–1462. https://doi.org/10.1016/j.gca.2006.12.009

D'Amore, D. V., Edwards, R. T., Herendeen, P. A., Hood, E., & Fellman, J. B. (2015). Dissolved organic carbon fluxes from hydropedologic units in Alaskan coastal temperate rainforest watersheds. *Soil Science Society of America Journal*, *79*(2), 378–388. https://doi.org/10.2136/sssaj2014.09.0380

Delbecq, C., Fellman, J. B., Bellmore, J. R., Whitney, E. J., Hood, E., Fitzgerald, K. A., & Falke, J. A. (2024). Seasonal patterns in riverine carbon form and export from a temperate forested watershed in Southeast Alaska. *Biogeochemistry*, *167*(11), 1353–1369. https://doi.org/10.1007/s10533-024-01175-7

Dinsmore, K. J., Billett, M. F., Dyson, K. E., Harvey, F., Thomson, A. M., Piirainen, S., & Kortelainen, P. (2011). Stream water hydrochemistry as an indicator of carbon flow paths in Finnish peatland catchments during a spring snowmelt event. *Science of the Total Environment*, *409*(22), 4858–4867. https://doi.org/10.1016/j.scitotenv.2011.07.063

Doctor, D. H., Kendall, C., Sebestyen, S. D., Shanley, S. B., Ohte, N., & Boyer, E. W. (2008). Carbon isotope fractionation of dissolved inorganic carbon (DIC) due to outgassing of carbon dioxide from a headwater stream. *Hydrological Processes*, *22*(1), 2410–2423. https://doi.org/10.1002/hyp.6833

Douglas, T. A., Blum, J. D., Guo, L., Keller, K., & Gleason, J. D. (2013). Hydrogeochemistry of seasonal flow regimes in the Chena River, a subarctic watershed draining discontinuous permafrost in interior Alaska (USA). *Chemical Geology*, *335*, 48–62. https://doi.org/10.1016/j.chemgeo.2012.10.045

Downing, B. D., Pellerin, B. A., Bergamaschi, B. A., Saraceno, J. F., & Kraus, T. E. C. (2012). Seeing the light: The effects of particles, dissolved materials, and temperature on in situ measurements of DOM fluorescence in rivers and streams. *Limnology & Oceanography*, *10*(10), 767–775. https://doi.org/10.4319/lom.2012.10.767

Ducharme, A. A., Casson, N. J., Higgins, S. N., & Friesen-Hughes, K. (2021). Hydrological and catchment controls on event-scale dissolved organic carbon dynamics in boreal headwater streams. *Hydrological Processes*, *35*(7), e14279. https://doi.org/10.1002/hyp.14279

Duvert, C., Bossa, M., Tyler, K. J., Wynn, J. G., Munksgaard, N. C., Bird, M. I., et al. (2019). Groundwater-derived DIC and carbonate buffering enhance fluvial CO2 evasion in two Australian tropical rivers. *Journal of Geophysical Research: Biogeosciences*, *124*(2), 312–327. https://doi.org/10.1029/2018JG004912

Duvert, C., Butman, D. E., Marx, A., Ribolzi, O., & Hutley, L. B. (2018). CO_2 evasion along streams driven by groundwater inputs and geomorphic controls. *Nature Geoscience*, *11*(11), 813–818. https://doi.org/10.1038/s41561-018-0245-y

Espinoza, V., Waliser, D. E., Guan, B., Lavers, D. A., & Ralph, F. M. (2018). Global analysis of climate change projection effects on atmospheric rivers. *Geophysical Research Letters*, *45*(9), 4299–4308. https://doi.org/10.1029/2017GL076968

Finlay, J., Neff, J., Zimov, S., Davydova, A., & Davydov, S. (2006). Snowmelt dominance of dissolved organic carbon in high-latitude watersheds: Implications for characterization and flux of river DOC. *Geophysical Research Letters*, *33*(10), L10401. https://doi.org/10.1029/2006GL025754

Gaillardet, J., Calmels, D., Romero-Mujalli, G., Zakharova, E., & Hartmann, J. (2019). Global climate control on carbonate weathering intensity. *Chemical Geology*, *527*, 118762. https://doi.org/10.1016/j.chemgeo.2018.05.009

Han Lu, Y., Bauer, J. E., Canuel, E. A., Chambers, R. M., Yamashita, Y., Jaffé, R., & Barrett, A. (2014). Effects of land use on sources and ages of inorganic and organic carbon in temperate headwater streams. *Biogeochemistry*, *119*(1–3), 275–292. https://doi.org/10.1007/s10533-014-9965-2

Hood, E., Gooseff, M. N., & Johnson, S. L. (2006). Changes in the character of stream water dissolved organic carbon during flushing in three small watersheds, Oregon. *Journal of Geophysical Research*, *111*(1), G01007. https://doi.org/10.1029/2005JG000082

Jantze, E. J., Laudon, H., Dahlke, H. E., & Lyon, S. W. (2015). Spatial variability of dissolved organic and inorganic carbon in subarctic headwater streams. *Arctic Antarctic and Alpine Research*, *47*(3), 529–546. https://doi.org/10.1657/AAAR0014-044

Johnson, M. S., Couto, E. G., Abdo, M., & Lehmann, J. (2011). Fluorescence index as an indicator of dissolved organic carbon quality in hydrologic flowpaths of forested tropical watersheds. *Biogeochemistry*, *105*(1), 149–157. https://doi.org/10.1007/s10533-011-9595-x

Jung, B. J., Lee, H. J., Jeong, J. J., Owen, J., Kim, B., Meusburger, K., et al. (2012). Storm pulses and varying sources of hydrologic carbon export from a mountainous watershed. *Journal of Hydrology*, *440–441*, 90–101. https://doi.org/10.1016/j.jhydrol.2012.03.030

Kaiser, K., & Kalbitz, K. (2012). Cycling downwards - Dissolved organic matter in soils. *Soil Biology and Biochemistry*, *52*, 29–32. https://doi.org/10.1016/j.soilbio.2012.04.002

Koch, J. C., Dornblaser, M. M., & Striegl, R. G. (2021). Storm-scale and seasonal dynamics of carbon export from a nested subarctic watershed underlain by permafrost. *Journal of Geophysical Research: Biogeosciences*, *126*(8), e2021JG006268. https://doi.org/10.1029/2021JG006268

Lader, R., Bhatt, U. S., Walsh, J. E., & Bieniek, P. A. (2022). Projections of hydroclimatic extremes in Southeast Alaska under the RCP8.5 scenario. *Earth Interactions*, *26*(1), 180–194. https://doi.org/10.1175/EI-D-21-0023.1

Lader, R., Bidlack, A., Walsh, J. E., Bhatt, U. S., & Bieniek, P. A. (2020). Dynamical downscaling for Southeast Alaska: Historical climate and future projections. *Journal of Applied Meteorology and Climatology*, *59*(10), 1607–1623. https://doi.org/10.1175/JAMC-D-20-0076.1

Leach, J. A., Larsson, A., Wallin, M. B., Nilsson, M. B., & Laudon, H. (2016). Twelve year interannual and seasonal variability of stream carbon export from a boreal peatland catchment. *Journal of Geophysical Research: Biogeosciences*, *121*(7), 1851–1866. https://doi.org/10.1002/2016JG003357

Li, S. L., Liu, C. Q., Li, J., Lang, Y. C., Ding, H., & Li, L. (2010). Geochemistry of dissolved inorganic carbon and carbonate weathering in a small typical karstic catchment of Southwest China: Isotopic and chemical constraints. *Chemical Geology*, *277*(3–4), 301–309. https://doi.org/10.1016/j.chemgeo.2010.08.013

Li, X., Wang, J., Lin, J., Yin, W., Shi, Y. Y., Wang, L., et al. (2022). Hysteresis analysis reveals dissolved carbon concentration – Discharge relationships during and between storm events. *Water Research*, *226*, 119220. https://doi.org/10.1016/j.watres.2022.119220

Lloyd, C. E. M., Freer, J. E., Johnes, P. J., & Collins, A. L. (2016a). Using hysteresis analysis of high-resolution water quality monitoring data, including uncertainty, to infer controls on nutrient and sediment transfer in catchments. *Science of the Total Environment*, *543*, 388–404. https://doi.org/10.1016/j.scitotenv.2015.11.028

Lloyd, C. E. M., Freer, J. E., Johnes, P. J., & Collins, A. L. (2016b). Technical Note: Testing an improved index for analyzing storm discharge-concentration hysteresis. *Hydrology and Earth System Sciences*, *20*(2), 625–632. https://doi.org/10.5194/hess-20-625-2016

McMillan, S. K., Wilson, H. F., Tague, C. L., Hanes, D. M., Inamdar, S., Karwan, D. L., et al. (2018). Before the storm: Antecedent conditions as regulators of hydrologic and biogeochemical response to extreme climate events. *Biogeochemistry*, *141*(3), 487–501. https://doi.org/10.1007/s10533-018-0482-6

Method 2320. Standard Methods for the Examination of Water and Wastewater. (1999). American Public Health Association.

Moatar, F., Abbott, B. W., Minaudo, C., Curie, F., & Pinay, G. (2017). Elemental properties, hydrology, and biology interact to shape concentration-discharge curves for carbon, nutrients, sediment, and major ions. *Water Resources Research*, *53*(2), 1270–1287. https://doi.org/10.1002/2016WR019635

Musselman, K. N., Lehner, F., Ikeda, K., Clark, M. P., Prein, A. F., Lui, C., et al. (2018). Projected increases and shifts in rain-on-snow flood risk over western North America. *Nature Climate Change*, *8*(9), 808–812. https://doi.org/10.1038/s41558-018-0236-4

Palecki, M., Durre, I., Applequist, S., Arguez, A., & Lawrimore, J. (2021). *U.S. climate normals 2020: U.S. hourly climate normals (1991-2020). JUNEAU INTL AP, AK US USW00025309*. NOAA National Centers for Environmental Information.

Perdrial, J. N., McIntosh, J., Harpold, A., Brooks, P. D., Zapata-Rios, X., Ray, J., et al. (2014). Stream water carbon controls in seasonally snow-covered mountain catchments: Impact of inter-annual variability of water fluxes, catchment aspect and seasonal processes. *Biogeochemistry*, *118*(1–3), 273–290. https://doi.org/10.1007/s10533-013-9929-y

Raymond, P. A., & Saiers, J. E. (2010). Event controlled DOC export from forested watersheds. *Biogeochemistry*, *100*(1), 197–209. https://doi.org/10.1007/s10533-010-9416-7

Sakamoto, T., Takahashi, M., Terajima, T., Nakai, Y., & Matsuura, Y. (1999). Comparison of the effects of rainfall and snowmelt on the carbon discharge of a small, steep, forested watershed in Hokkaido, northern Japan. *Hydrological Processes*, *13*(14–15), 2301–2314. https://doi.org/10.1002/(sici)1099-1085(199910)13:14/15<2301::aid-hyp876>3.0.co;2-u

Sanderman, J., Lohse, K. A., Baldock, J. A., & Amundson, R. (2009). Linking soils and streams: Sources and chemistry of dissolved organic matter in a small coastal watershed. *Water Resources Research*, *45*(3), W03418. https://doi.org/10.1029/2008WR006977

Saraceno, J. F., Pellerin, B. A., Downing, B. D., Boss, E., Bachand, P. A. M., & Bergamaschi, B. A. (2009). High-frequency in situ optical measurements during a storm event: Assessing relationships between dissolved organic matter, sediment concentrations, and hydrologic processes. *Journal of Geophysical Research*, *114*(4), G00F09. https://doi.org/10.1029/2009JG000989

Saraceno, J. F., Shanley, J. B., Downing, B. D., & Pellerin, B. A. (2017). Clearing the waters: Evaluating the need for site-specific field fluorescence corrections based on turbidity measurements. *Limnology and Oceanography: Methods*, *15*(4), 408–416. https://doi.org/10.1002/lom3.10175

Schlesinger, W. H., & Bernhardt, E. S. (2020). *Biogeochemistry: An analysis of global change* (4th ed.). Elsevier/Academic Press.

Sergeant, C. J., Falke, J. A., Bellmore, R. A., Bellmore, J. R., & Crumley, R. L. (2020). A classification of streamflow patterns across the coastal Gulf of Alaska. *Water Resources Research*, *56*(2), e2019WR026127. https://doi.org/10.1029/2019WR026127

Singh, S., Inamdar, S., Mitchell, M., & McHale, P. (2014). Seasonal pattern of dissolved organic matter (DOM) in watershed sources: Influence of hydrologic flow paths and autumn leaf fall. *Biogeochemistry*, *118*(1–3), 321–337. https://doi.org/10.1007/s10533-013-9934-1

Speir, S. L., Rose, L. A., Blaszczak, J. R., Kincaid, D. W., Fazekas, H. M., Webster, A. J., et al. (2023). Catchment concentration–discharge relationships across temporal scales: A review. *WIREs Water*, *11*(2), e1702. https://doi.org/10.1002/wat2.1702

Su, H., Cheng, L., Wu, Y., Qin, S., Liu, P., Zhang, Q., et al. (2023). Extreme storm events shift DOC export from transport-limited to source-limited in a typical flash flood catchment. *Journal of Hydrology*, *620*, 129377. https://doi.org/10.1016/j.jhydrol.2023.129377

Tank, S. E., Fellman, J. B., Hood, E., & Kritzberg, E. S. (2018). Beyond respiration: Controls on lateral carbon fluxes across the terrestrial-aquatic interface. *Limnology and Oceanography Letters*, *3*(3), 76–88. https://doi.org/10.1002/lol2.10065

Vaughan, M. C. H., Bowden, W. B., Shanley, J. B., Vermilyea, A., & Schroth, A. W. (2019). Shining light on the storm: In-stream optics reveal hysteresis of dissolved organic matter character. *Biogeochemistry*, *143*(3), 275–291. https://doi.org/10.1007/s10533-019-00561-w

Vaughan, M. C. H., Bowden, W. B., Shanley, J. B., Vermilyea, A., Sleeper, R., Gold, A. J., et al. (2017). High-frequency dissolved organic carbon and nitrate measurements reveal differences in storm hysteresis and loading in relation to land cover and seasonality. *Water Resources Research*, *53*(7), 5345–5363. https://doi.org/10.1002/2017WR020491

Ward, N. D., Bianchi, T. S., Medeiros, P. M., Seidel, M., Richey, J. E., Keil, R. G., & Sawakuchi, H. O. (2017). Where carbon goes when water flows: Carbon cycling across the aquatic continuum. *Frontiers in Marine Science*, *4*(7). https://doi.org/10.3389/fmars.2017.00007

Wen, H., Sullivan, P. L., Billings, S. A., Ajami, H., Cueva, A., Flores, A., et al. (2022). From soils to streams: Connecting terrestrial carbon transformation, chemical weathering, and solute export across hydrological regimes. *Water Resources Research*, *58*(7), e2022WR032314. https://doi.org/10.1029/2022WR032314

Wiegner, T. N., Tubal, R. L., & MacKenzie, R. A. (2009). Bioavailability and export of dissolved organic matter from a tropical river during base- and stormflow conditions. *Limnology & Oceanography*, *54*(4), 1233–1242. https://doi.org/10.4319/lo.2009.54.4.1233

Williams, G. P. (1989). Sediment concentration versus water discharge during single hydrologic events in rivers. *Journal of Hydrology*, *111*(1–4), 89–106. https://doi.org/10.1016/0022-1694(89)90254-0

Wilson, H. F., Saiers, J. E., Raymond, P. A., & Sobczak, W. V. (2013). Hydrologic drivers and seasonality of dissolved organic carbon concentration, nitrogen content, bioavailability, and export in a forested New England stream. *Ecosystems*, *16*(4), 604–616. https://doi.org/10.1007/s10021-013-9635-6

Yamashita, Y., Kloeppel, B. D., Knoepp, J., Zausen, G. L., & Jaffé, R. (2011). Effects of watershed history on dissolved organic matter characteristics in headwater streams. *Ecosystems*, *14*(7), 1110–1122. https://doi.org/10.1007/s10021-011-9469-z

Zarnetske, J. P., Bouda, M., Abbott, B. W., Saiers, J., & Raymond, P. A. (2018). Generality of hydrologic transport limitation of watershed organic carbon flux across ecoregions of the United States. *Geophysical Research Letters*, *45*(21), 702–711. https://doi.org/10.1029/2018GL080005